Celestial Mechanics and Dynamical Astronomy (2005) 92:257–272
DOI 10.1007/s10569-005-2064-x

THE ROLE OF HYPERBOLIC INVARIANT SETS IN STICKINESS EFFECTS

YI-SUI SUN[1], LI-YONG ZHOU[1,2] and JI-LIN ZHOU[1]
[1]*Department of Astronomy, Nanjing University, Nanjing 210093, China, e-mail: sunys@nju.edu.cn*
[2]*Tuorla Observatory, Väisäläntie 20, Piikkiö 21500, Finland*

(Received: 21 June 2004; revised: 28 December 2004; accepted: 10 February 2005)

Abstract. With the standard map model, we study the stickiness effect of invariant tori, particularly the role of hyperbolic sets in this effect. The diffusion of orbits originated from the neighborhoods of hyperbolic points, periodic islands and torus is studied. We find that they possess similar diffusion rules, but the diffusion of orbits originated from the neighborhood of a torus is faster than that originated near a hyperbolic set. The numerical results show that an orbit in the neighborhood of a torus spends most of time around hyperbolic invariant sets. We also calculate the areas of islands with different periods. The decay of areas with the periods obeys a power law, and the absolute values of the exponents increase monotonously with the perturbation parameter. According to the results obtained, we conclude that the stickiness effect of tori is caused mainly by the hyperbolic invariant sets near the tori, and the diffusion speed becomes larger when orbits diffuse away from the torus.

Key words: hyperbolic invariant sets, invariant tori, stickiness effect

1. Introduction

Hamiltonian systems are conservative dynamical systems which are encountered in various areas. The phase space of a nearly integrable Hamiltonian system typically consists of regular and chaotic regions. The study of orbital diffusion in the phase space is the basis of many topics in Hamiltonian dynamics. A chaotic orbit initialized close to a KAM torus will wander for a long time before it finally leaves the vicinity of the torus. Since Karney (1983) first uses the term "sticky" to describe such effect around islands, this phenomenon was then called the "stickiness effect" of invariant tori. The study of stickiness effect has now been extended to include all kinds of effects which slow down the diffusion. These effects may come from different invariant sets such as invariant tori (Lai et al., 1992; Perry and Wiggins, 1994; Sun and Fu, 1999), island-chains (Karney, 1983; Chirikov and Shepelyansky, 1984; Sun et al., 2002) and Cantori (Meiss and Ott, 1985; Contopoulos et al., 1997). We call this extended concept the "generalized stickiness effect". Moreover, it is also known that hyperbolic invariant sets possess the stickiness effect too (Froeschlé and Lega, 1998; Contopoulos et al., 1999; Zhou et al., 2002).

Zhou et al. (2002) suggested that the hyperbolic invariant sets is essential to the stickiness effect. In this paper we will clarify and confirm numerically this conclusion with the standard map model.

2. Model

We take the standard map T as the model,

$$T: \begin{cases} x_{n+1} = x_n + y_{n+1} \\ y_{n+1} = y_n - \frac{k}{2\pi}\sin(2\pi x_n) \end{cases} (\text{mod } 1), \tag{1}$$

where k is the perturbation parameter. Figure 1 is the diagram of map T with $k = 1$.

We choose an island from the period-5 island-chain (indicated by the arrow in Figure 1) as the chief torus to analyze. The center of the chief torus is at $(x_0, y_0) = (0.2476544, 0.6638289)$. Figure 2 is the enlargement of the chief torus, around which come out islands and hyperbolic invariant sets with different orders due to the self-similarity. In the following sections, we will investigate the stickiness effect of the chief torus as well as of the periodic islands and the hyperbolic invariant sets near it. The role of the hyperbolic invariant sets in the generalized stickiness effect will be discussed in detail.

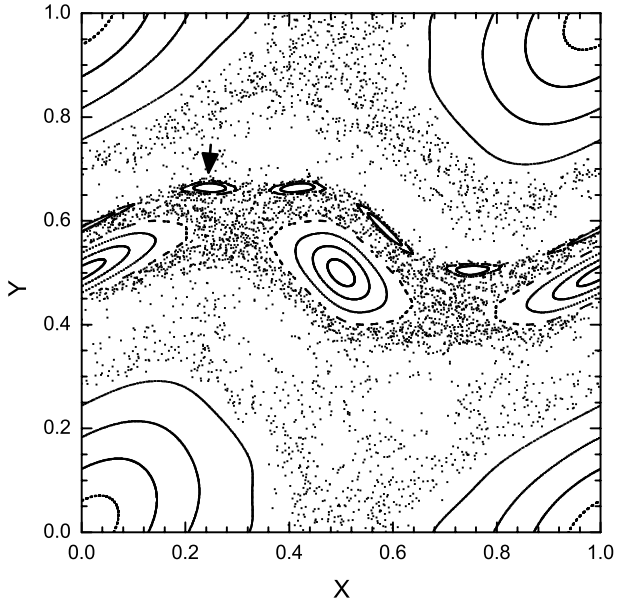

Figure 1. Phase diagram of map T with $k = 1.0$.

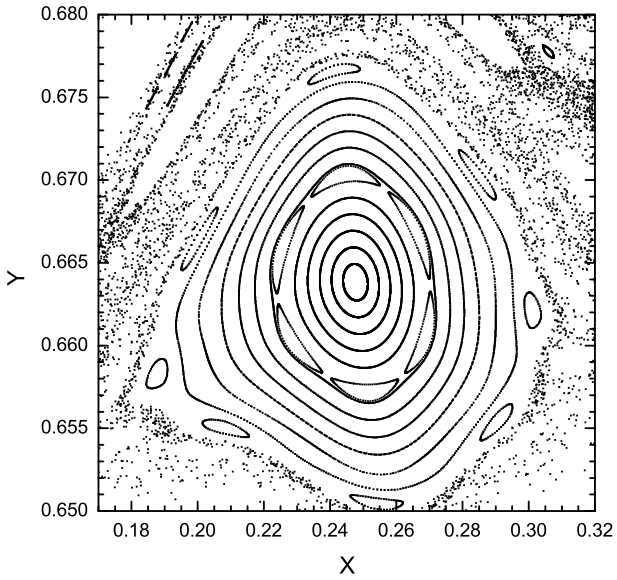

Figure 2. Enlargement of one island (called the chief torus in the paper) from the period-5 island-chain.

3. Numerical Results

3.1. STICKINESS EFFECT OF HYPERBOLIC INVARIANT SETS

From Figure 3 we can see that in the vicinity of the chief torus, there is an island-chain with 23 periodic islands and a hyperbolic invariant set consisting of 23 periodic hyperbolic fixed points as predicted by the Poincaré-Birkhoff fixed point theorem. We investigate the stickiness effect of this hyperbolic invariant set.

To study the stickiness effect of the hyperbolic invariant set, we trace an orbit with an initial point $(x, y) = (0.2972650, 0.6591000)$, which is very close to one of the period-23 hyperbolic fixed points $(x_h, y_h) = (0.2972704, 0.6590667)$. Figure 4 shows the diffusion process of the orbit. Because the orbit diffuses to a secondary island-chain (or a secondary hyperbolic invariant set) when the iterative number $n \sim 3 \times 10^5$, we trace the orbit up to $n = 2 \times 10^5$ iterations, before that the orbit diffuses around the hyperbolic invariant set. Since the orbit is very close to the "boundary" of the chief torus, we can calculate the distribution of points on the orbit along the "boundary", which can be approximatively defined as the possible outermost curve l of the chief torus. Every point near l can be projected to l, so that gets a reference coordinate from the projection on l. In such a way we can see where the orbit is "stuck" during its diffusion.

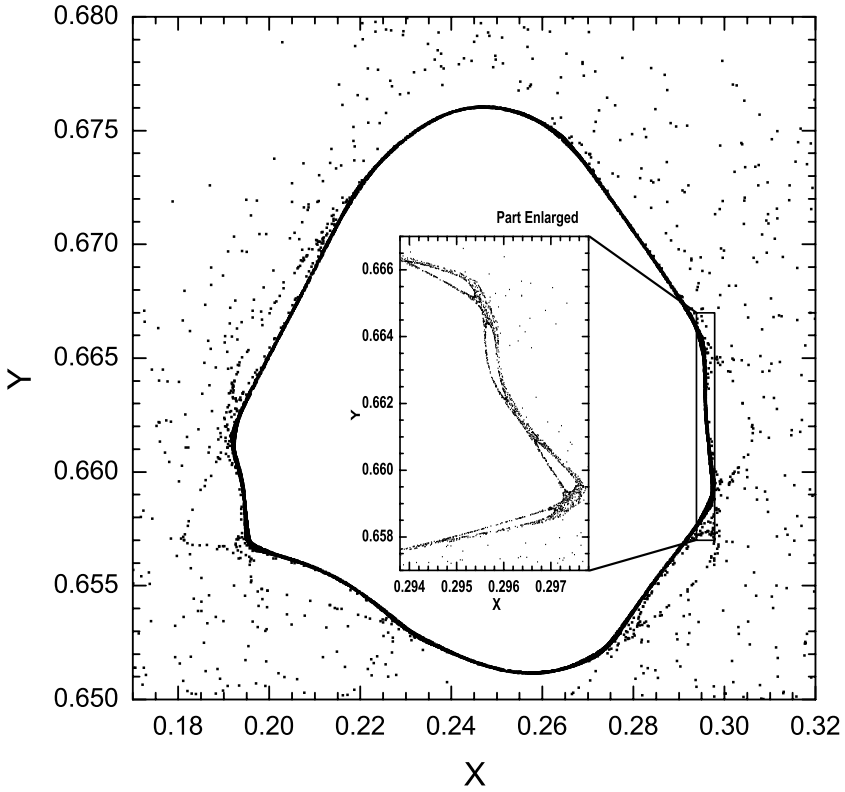

Figure 3. Diagram of the period-23 secondary islands around the chief torus.

In Figure 5 we show the distribution of orbit points with respect to the length of l, and the positions of the 23 hyperbolic fixed points are marked too. The outstanding feature of Figure 5 is that every peak evidently corresponds just to one of the positions of the period-23 hyperbolic fixed points (hyperbolic invariant set). The distribution of points on other orbits starting from points not very close to the hyperbolic fixed point, but lying between two neighboring hyperbolic fixed points in the same hyperbolic invariant set, are found to have very similar distribution to the one in Figure 5. We repeated the same calculation around a higher-order island (one of the 23 islands around the chief torus), and obtained the same results as above.

Now it should be stressed that an orbit spreads in fact in a 2-dimensional zone, so that the density of orbit points in the sticky zone should be counted in definite areas rather than along a curve. However, from a practical view, there is no straightforward method to define such areas, in which higher-order islands are embedded as holes and around them there are secondary hyperbolic invariant sets related with the stickiness effects of the

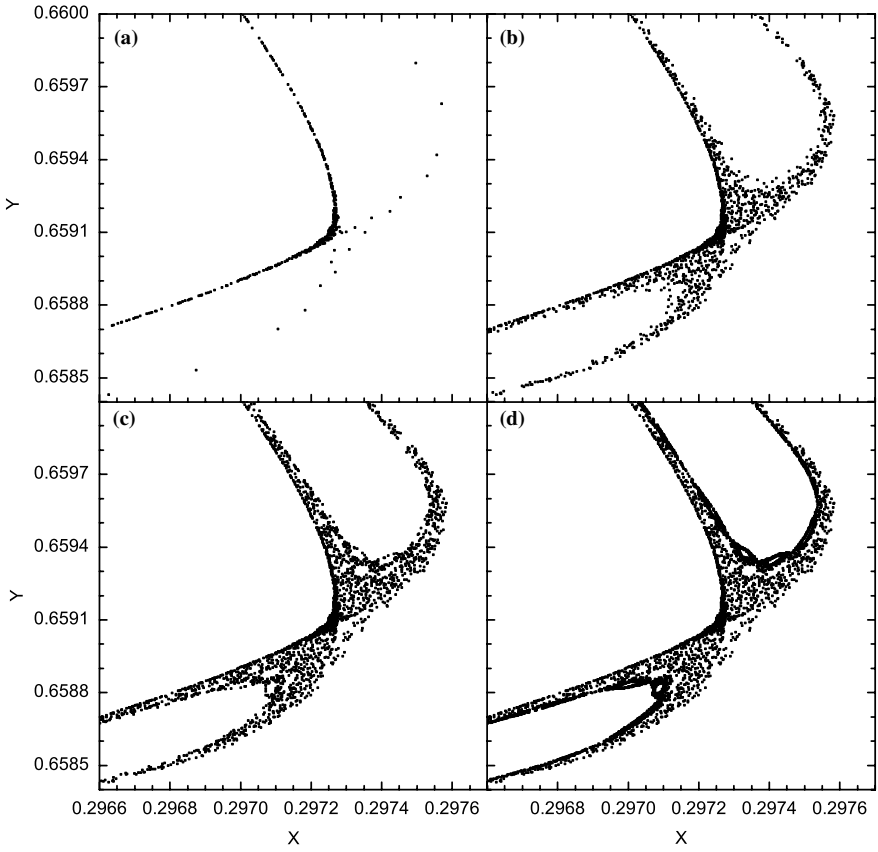

Figure 4. Diffusion of an orbit around a hyperbolic invariant fixed point. a, b, c and d are the snapshots of the orbit up to 5×10^4, 2×10^5, 3×10^5 and 6×10^5 iterations, respectively.

higher-order islands. On the other hand, the sticky zone occupied by an orbit shown in Figure 4 as an example shows a little thinner width around the hyperbolic points than around the rest of the zone, and in fact, from Figure 4 we can see that the orbit points near the hyperbolic fixed point are denser than in the zones far from it. Therefore, even if the sticky zone is considered roughly as a uniformly wide strip around the chief torus, the distribution along a curve in Figure 5 would reflect approximately the distribution of orbit points in the sticky area near the chief torus.

It is well known that there are many different unstable periodic orbits in a chaotic region. In Figure 5 the match between the positions of the outstanding peaks and the hyperbolic fixed points reveals that this hyperbolic invariant set is much more important than others in this region. It also implies that such orbits spend more time around this hyperbolic invariant set than elsewhere, therefore the hyperbolic invariant set plays an important role

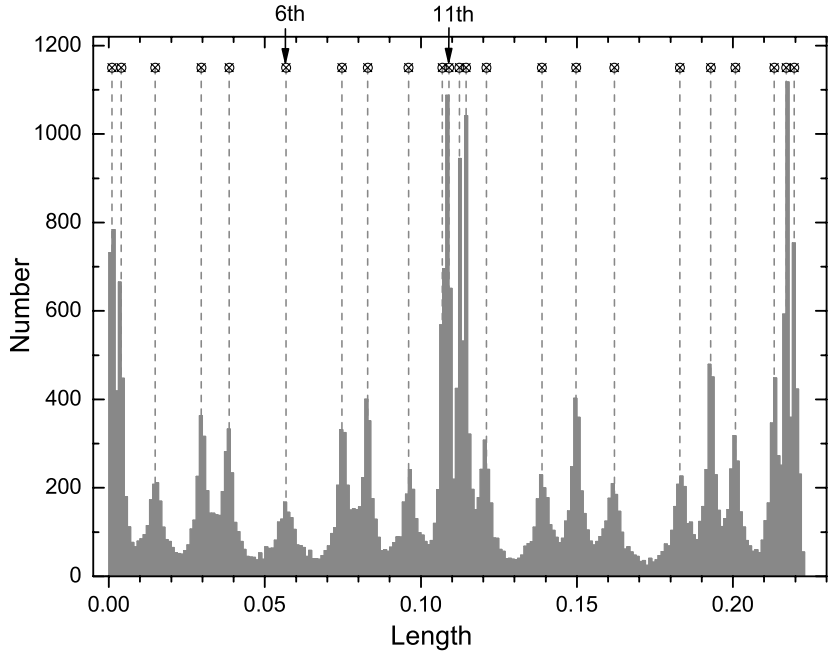

Figure 5. Distribution of points on orbit. The crosses inside circles correspond to the positions of the 23 hyperbolic fixed points.

in the stickiness effects. Moreover, an orbit on the "outermost" invariant curve also has a similar accumulation of points (the distribution is very similar to Figure 5). Since this invariant curve is very close to the hyperbolic set located among the island-chain, this accumulation can be explained by the continuous dependence of the density of orbits on the initial conditions.

We note the peaks in Figure 5 have different heights. With the eigenvalues and eigenvectors of the mapping on the hyperbolic points, it may be given an explanation. By iterating 115 ($= 5 \times 23$) times of the tangent map of (1), we get the matrix of the corresponding tangent map and then calculate the eigenvalues and eigenvectors of this matrix. The results show that for a hyperbolic point corresponding to a higher peak, the angle between eigenvectors (standing for directions of stable and unstable manifold at this point) is relatively bigger, and the eigenvalue corresponding to the unstable direction has a smaller value. While on a lower peak, the angle is smaller and the eigenvalue is bigger. For instance, the eigenvalues and eigenvectors of the sixth (counting from left to right, indicated by an arrow in Figure 5) hyperbolic points, which has a lower peak, are $\lambda_1 = 20.1326, \mathbf{v}_1 = (1.00000, -1.23649 \times 10^{-4})^T$; $\lambda_2 = 4.96707 \times 10^{-2}, \mathbf{v}_2 = (0.998415, 5.62761 \times 10^{-2})^T$. The angle between $\mathbf{v}_1$ and $\mathbf{v}_2$ is $\alpha = 3^\circ.23345$. In comparison, for the 11th point in Figure 5, which possesses a higher peak, we have $\lambda_1' = 3.84879, \mathbf{v}_1' = (-0.687897, -0.725808)^T$;

$\lambda_2' = 0.259822, \mathbf{v}_2' = (-0.841136,\ 0.540823)^T$; and $\alpha' = 79°.2758$. The same phenomena appear in the case of other hyperbolic points. In the case of a lower peak, the orbit spreads quickly due to the bigger eigenvalue λ_1 in the unstable direction and occupies a wide region along the invariant curve. While in the case with a higher peak, orbit diffuses along the unstable direction in a relatively smaller speed ($\lambda_1' < \lambda_1$), and the points of an orbit focus in a relatively narrower region ($\alpha' > \alpha$). Consequently, the peaks have different heights.

3.2. STICKINESS EFFECT OF TORI

In order to clarify further the role of hyperbolic invariant sets in the stickiness effect of tori, we discuss the diffusion of orbits in the vicinity of tori. We define a "neighboring zone" of the torus, and if an orbit diffuses away from this zone, we regard it as "escaped". To do this, we first calculate the length L of the boundary curve l of the chief torus and the area A surrounded by it. Then we define the neighboring zone around the chief torus by expanding the curve l outwards a width $D = (A/10L)$, i.e., the area of the neighboring zone is taken as $A/10$, where $A = 1.8341447 \times 10^{-3}$, $L = 0.2221069$. As soon as the distance of an orbit to the chief torus is larger than $2D$, we regard it as escaped.

3.2.1. *Diffusion of orbits near the chief torus*

We take 20,000 initial points spread uniformly in the neighboring zone of the chief torus, P_0^{ij}: $(r_0^i + (j/20)D, \theta_0^i = (2\pi/1000)i)$, $i = 1, 2, \ldots, 1000, j = 1, 2, ..., 20$, where (r_0^i, θ_0^i) are the polar coordinates of the points P_0^i on l. Then we choose 2000 points $P_c^k = (r_c^k, \theta_c^k)$, $k = 1, 2, \ldots, 2000$ spread uniformly on l as the standard points. After n iterations of the map T, a point P_m^{ij} ($m = (n/5)$, noting the period 5) on the orbit initialized from point P_0^{ij} is regarded as escaped, if the distance $d = \min(P_c^k, P_m^{ij}) > 2D$, where $1 \leqslant k \leqslant 2000$. We regard an orbit as never escaped if it is not escaped before $n = 1.15 \times 10^7$. In the same way we take another 20,000 initial points near one of the 23 periodic hyperbolic fixed points $(x_h, y_h) = (0.2972704, 0.6590667)$. The selected initial points are all in a segment of the above mentioned neighboring zone with angle coordinates from $\theta_1 = 6.1851$ to $\theta_2 = 6.1903$. Interpretatively, this fixed point and its two neighboring fixed points respectively have angle coordinates of $\theta = 6.1875$, 6.1478 and 6.2337. With the above definitions, we illustrate in Figure 6 the variations of the surviving orbit number with time (iteration number) for both cases. From Figure 6 we see the two curves are very similar, but for the orbits starting

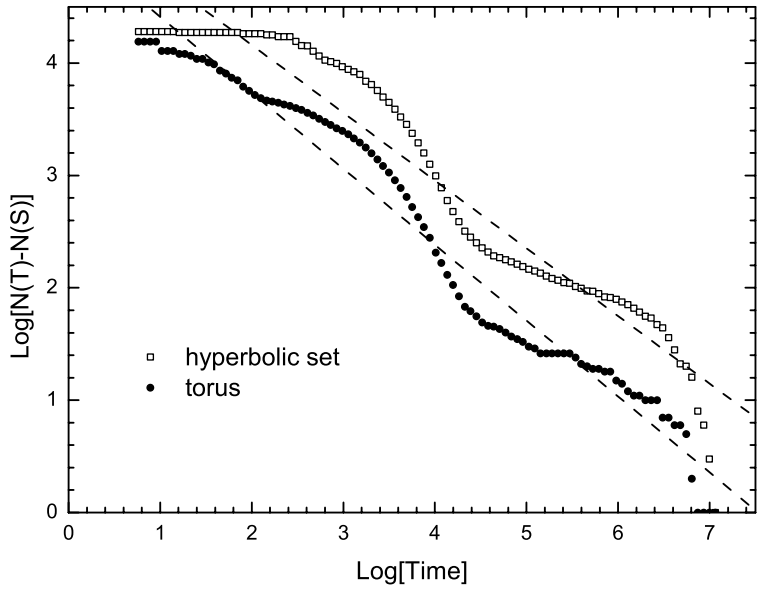

Figure 6. Diffusion of orbits started closed to the chief torus and close to the hyperbolic fixed point. The total number of points that have not escaped at time T is denoted by $N(T)$ and the number of points that will never escape is denoted by $N(S)$. Dots and squares stand for the cases close to the chief torus and close to the hyperbolic fixed points, respectively. The dashed lines are the linear fittings.

near the hyperbolic fixed point, the diffusion is slower than those started from the vicinity of the chief torus.

Two different quantities can quantify the stickiness effect: the exponent of the power law of orbit diffusion and the average time of orbit escape. According to the results shown by Ding et al. (1990), the surviving number N of orbits starting from a mixed region in the phase space of a Hamiltonian system will decrease in a power law with respect to time T: $N \sim T^{-z}$, where z is a positive number depending on the dimension D of the system. When $D = 2$, $z = 1.2 \sim 1.5$. In our cases, we find that each curve in Figure 6 can be divided into several segments, which can be linearly fitted with different slopes. Particularly, when $\log[\text{Time}] \in [3.6, 4.4]$ both of the two curves can be well fitted by lines with slopes of -1.5, that is, the exponent here is $z = 1.5$. Besides, there are segments with smaller z, and we also find $z = 3$ when $\log[\text{Time}] > 6.4$, which is consistent with the result in Chirikov and Shepelyansky (1999). Despite these interesting details, in this paper we focus mainly on the similar profiles of the two varying curves, therefore here we report the average exponents over the whole time range from 0 to 10^7, which are $z_1 = 0.6756$ and $z_2 = 0.6028$ respectively for both cases with starting points near the chief torus and the hyperbolic sets as mentioned above. The small

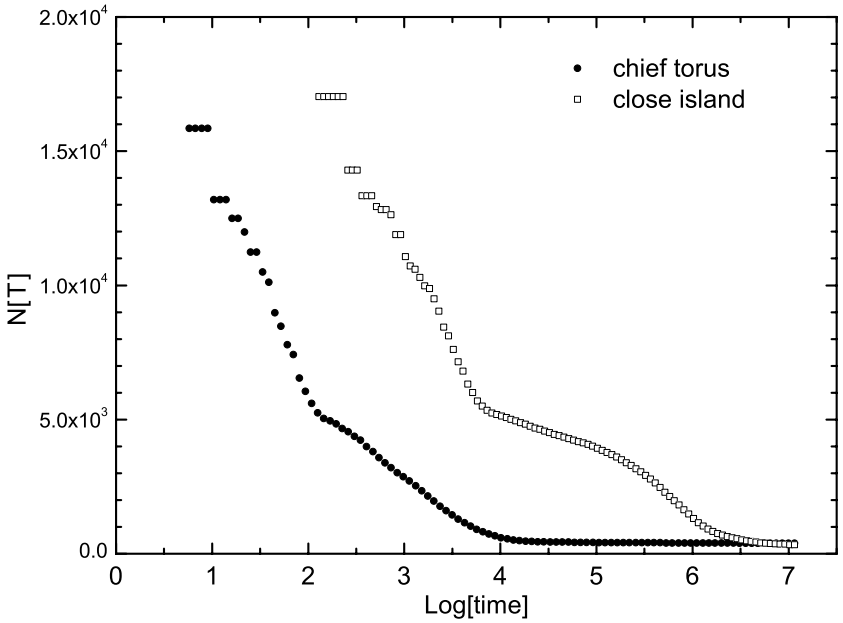

Figure 7. Diffusion of orbits started close to the chief torus and close to the island in the vicinity of the chief torus. Dots denote the case close to the chief torus, and squares denote the case close to the island.

values of z_1, z_2 are due to the existence of segments with flat slope. The average times of escape $\bar{T} = (1/N_0)\int_0^{N_0} T\,\mathrm{d}N$ are also numerically calculated and they are $\bar{T}_1 = 4815$ and $\bar{T}_2 = 18677$ (iteration times) for the cases of torus and hyperbolic set, respectively.

Both the exponent z and the average time of escape $\bar{T}$ imply that, the orbits with initial points in the vicinity of the chief torus, will diffuse faster than those started near the hyperbolic invariant set. These results also imply the hyperbolic invariant sets will play a major role in slowing down the diffusion of orbits near the torus, or in the stickiness effect of tori.

3.2.2. *Diffusion of orbits near the islands*

The phase space of map T possesses the self-similarity structure and an orbit may diffuse around islands of different orders on its way of escaping. In this section, we study the orbital diffusion near one of the above mentioned 23 periodic islands around the chief torus with center at $(x, y) = (0.2972144, 0.6599696)$. The neighboring zone and the escape criteria are the same as that in last subsection, but the A and L are now $A = 2.8499899 \times 10^{-7}$, $L = 3.0598743 \times 10^{-3}$. With the same way of taking initial points, we follow the evolution of 20,000 orbits starting from the

neighboring zone of this island. Figure 7 displays the diffusion of orbits near the island and near the chief torus as a comparison. The similarity between the profiles of the two curves in Figure 7 implies the similar sources of the stickiness effects in these two cases. Combined with Figure 6 we may argue once again that the stickiness effect of island is also caused mainly by the hyperbolic invariant set near it. By the way, Figure 7 does not mean that the diffusion speed of orbits near island is slower than that near the chief torus, because the definitions of the escaping zone of chief torus and island are only similar, but not the same.

3.3. SIZE OF ISLANDS

Froeschlé and Lega (1998) studied the variations of sizes of Fibonacci islands with the distance to the chief torus. Efthymiopoulos et al. (1997) discussed the variations of islands sizes with perturbation parameter. In this paper we measure the size of different islands including the chief torus in the phase space, then investigate the variations of islands' area with respect to the periods of island-chains and to the system perturbation parameter k. With these results we can understand further the orbital diffusion in phase space and the role of hyperbolic invariant sets in the stickiness effect of tori. Here the area of an island is approximated by the summation of areas of 2000 triangles inside the "outermost" invariant curve surrounding the island.

We compute the areas of islands of different periods (the chief torus is a period-5 island) in the main (island) sequences (island-chain sequence surrounding the central island) for $k = 0.90, 0.95, 1.00, 1.05$ and 1.10, respectively. The results are shown in Figure 8, in which each square denotes the total area of an island-chain of a definite period. From Figure 8 we can find that the decay of island area with respect to the period obeys roughly a power law, and the absolute values of the slopes of fitting lines increase monotonically with k. This means that the decay rate of the area for island sequences increases with the perturbation parameter k (Figure 9).

As well known, the self-similarity property indicates that there are secondary islands around an island in the main sequence, and then higher order islands around this secondary islands, and so on. To study the area of such "islands around islands", we select the most outstanding secondary island chain around an island, and successively repeat such selecting to higher and higher order. We call such an island sequence "hierarchical (island) sequence". Taking $k = 1.0$, we compute the areas of islands in several hierarchical sequences starting respectively from islands with periods of 4, 16 and 29 in the main sequence. The numerical results displayed in Figure 10 show

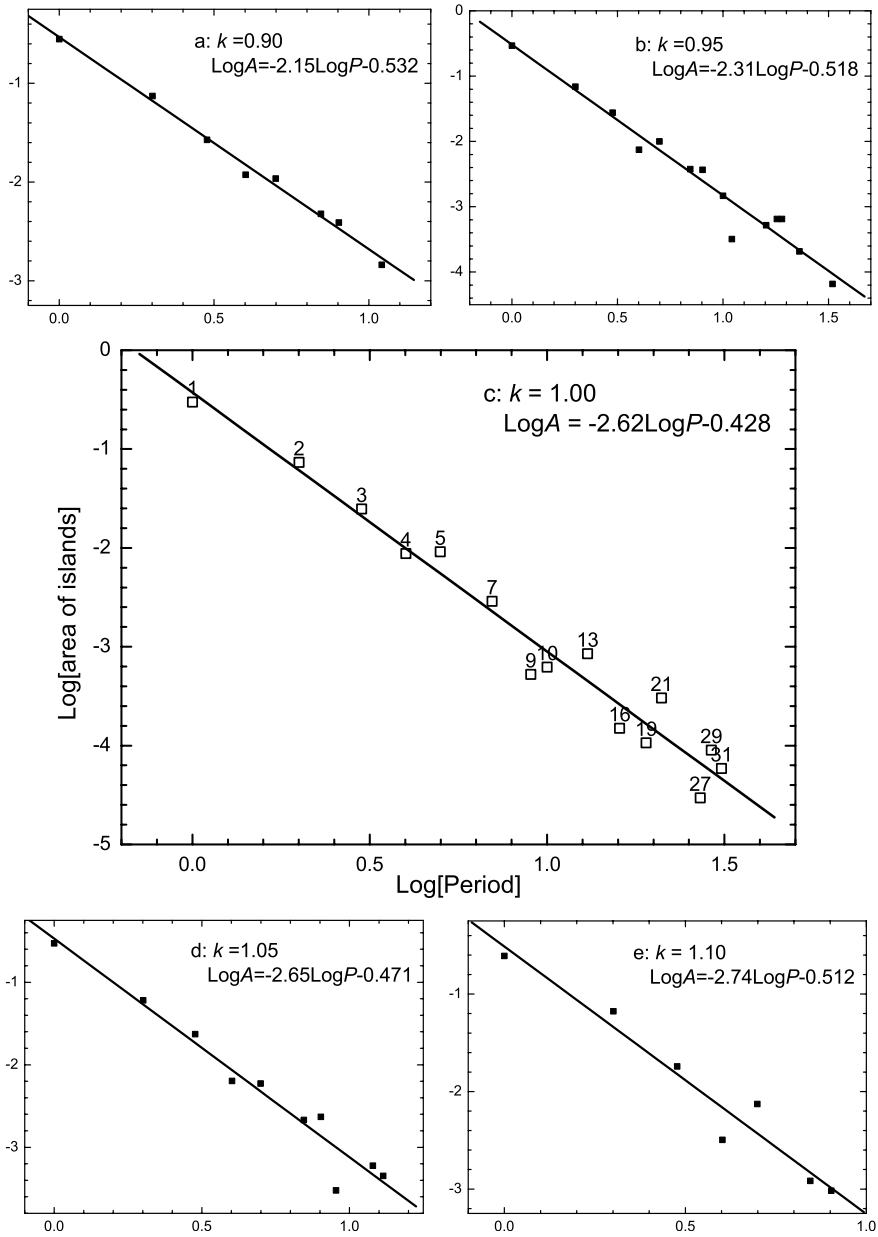

Figure 8. Variations of area of islands in the main island sequence with respect to the period of island. The linear fit of the data is indicated by both a line and a linear function. (a), (b), (c), (d) and (e) are the situations of $k = 0.90, 0.95, 1.00, 1.05$ and 1.10, respectively. The numbers above the squares in (c) denote the periods of corresponding islands.

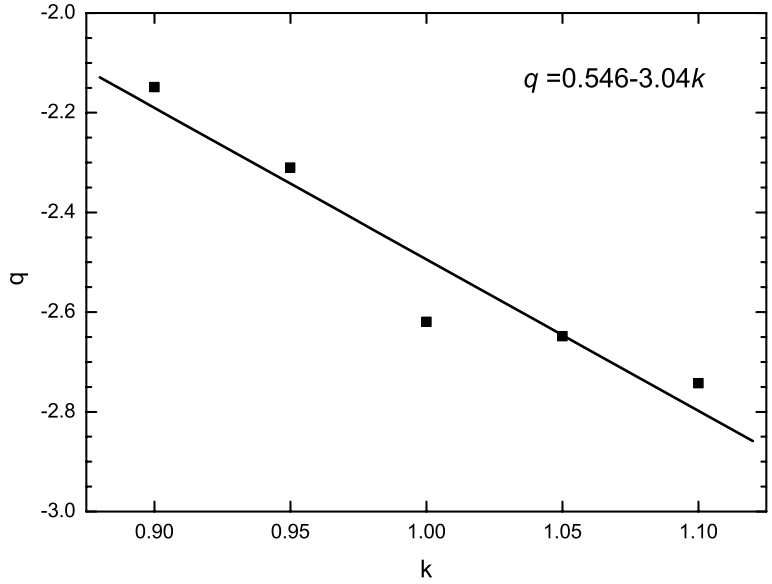

Figure 9. Variation of slopes q of fitting lines in Figure 9 with the perturbation parameter k.

the decay of the area of islands in the hierarchical sequence possesses a power law too, but compared with the case for main sequence, the absolute values of the slopes q of fitting lines are smaller. This implies the decay of areas in the hierarchical sequences is slower than that in the main sequence.

Efthymiopoulos et al. (1999) found that the sizes A of islands with odd and even "multiplicities" (periods) P in a sequence approaching to a cantorus decrease following the same power law $A = CP^{-2.75}$ but with different constants C. In this paper, we investigate the relations between the areas and the periods of islands in the main and the hierarchical island sequences, respectively. They are all proved to be power laws with different exponents. The variations of such exponents with respect to parameter k are also studied and we found that the exponents are the same for island sequences with even and odd periods provided the parameters k are the same.

Now we try to estimate the upper bound of the total area of islands in phase space. As indicated above, the variation of island area with period possesses roughly a power law, i.e. $\log A_{\mathrm{P}}(k) = q(k) \log P + C(k)$, where $A_{\mathrm{P}}(k)$ is the total area of period-P islands for a given k, $q(k)$ the slope and $A_1(k) = 10^{C(k)}$ the area of the central island (period-1 island). According to the result in Figure 9, we have $q(k) = 0.546 - 3.04k$ and $A_{\mathrm{P}}(k) = P^{0.546-3.04k} A_1(k)$, $P \in \{N\}$, while $\{N\}$ is the set of period of islands in the main sequence for $k \in [0.90, 1.10]$. Based on these we obtain the total area of islands in the main island sequence

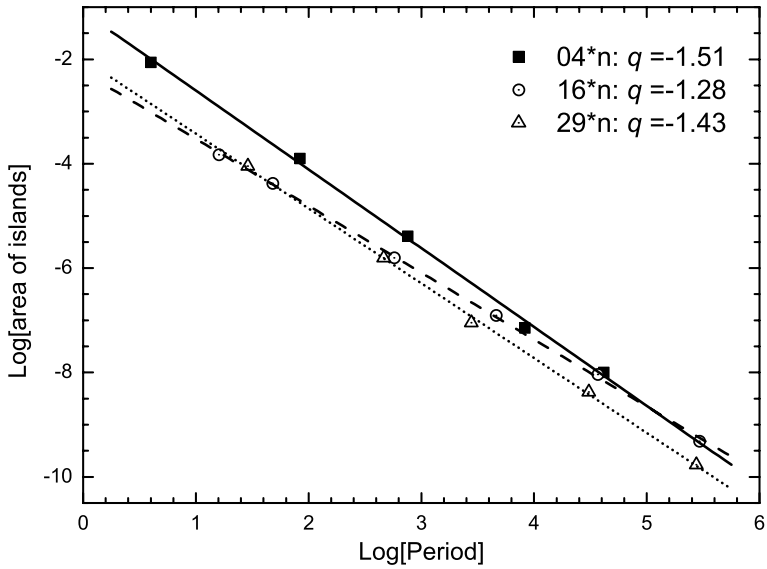

Figure 10. Variations of area of island in the hierarchical island sequences with the period of islands, and the corresponding fitting lines. The filled squares, circles and triangles represent the situations in the sequence starting from the period-4, 16, and 29 islands in the main sequence. q is the slope of the fitting line.

$$A(k) = \sum_{P\in\{N\}} A_{\mathrm{P}}(k) \leqslant \sum_{P\in[1,\infty)} A_{\mathrm{P}}(k) = A_1(k) \sum_{P\in[1,\infty)} P^{q(k)}. \tag{2}$$

We know that series $\sum_{n=1}^{\infty}(1/n^s)$ is convergent if $s > 1$, and the sum is called Riemann function $\zeta(s)$. After elementary calculus, we get

$$\zeta(s) < \frac{1 - s - 2^{-s}(1+s)}{1-s} = 1 - \frac{2^{-s}(1+s)}{1-s}. \tag{3}$$

Thus we have

$$A(k) < A_1(k)[1 - \frac{2^{q(k)}(1-q(k))}{1+q(k)}] = U(k), k \in [0.90, 1.10]. \tag{4}$$

Generally the area of central island decreases as k increases in a long term for large variation of k, but the varying is not smooth. It can even increase temporarily (Efthymiopoulos et al., 1997), as happening to occur in the present case. However we take the average $\overline{C}(k)$ for the five values of k, $\overline{C}(k) = -0.502$.

Substituting $q(k) = 0.546 - 3.04k$ and $A_1(k) = 10^{-0.502}$, we finally get an upper bound $U(k)$ of the total area of islands in the main island sequence. Because the total area of higher-order islands in the hierarchical island sequences is much smaller than that in the main island sequence, $U(k)$ is roughly an upper bound of the total area of islands in phase space. Calcu-

lating of Equation (4) shows $U(k) = 0.500, 0.469, 0.445, 0.426$, and 0.410 when $k = 0.90, 0.95, 1.00, 1.05$, and 1.10, respectively.

If there were more values of island area for large variation of k, and if we could get a better expressions on $q(k)$ and $C(k)$, we would have a better estimation of the upper bound of the total area of islands in phase space for given k.

On the other hand, the whole phase space in our model consists of islands and other invariant sets. If the total area of islands is smaller than 1.0, the residue of them must have a positive measure. This may also imply the importance of hyperbolic sets in the orbital diffusion. Although the above calculation is only a coarse estimate, we hope it can give some valuable hints.

4. Conclusions

From the above results, we conclude that:

(1) An orbit started close to tori will spend most of time near the hyperbolic invariant sets surrounding the tori, before escaping from the vicinity. This is reasonable because of the following fact: according to the character of the hyperbolic invariant set, an orbit would spend very long time in approaching to (leaving from) a hyperbolic fixed point along the stable (unstable) manifold.
(2) The orbits started close to tori and those started close to hyperbolic invariant sets obey the same diffusion rules, but in the latter case the orbits diffuse slower than that in the former case.
(3) For the orbits initially close to the chief torus and orbits initially close to the secondary island, respectively, they possess the similar diffusion rule. This is consistent with the character of self-similarity structure of phase space.
(4) The decay of island area with period in both the case of main island sequence and hierarchical island sequence obeys roughly a power law, and in the former case the absolute values of the slope of fitting line increase monotonously with k. From these results it seems that when an orbit diffuses outwards from the chief torus more and more, the probability of its encounter with the islands should be smaller and smaller, and this could be a reason for the gradually faster diffusion of an orbits farther from the chief torus. Moreover, the speed of diffusion increases with k, coinciding with the above conclusions.

Finally, we conclude that the stickiness effect of tori is indeed caused mainly by the hyperbolic invariant sets in the vicinity of tori. According to the Poincaré-Birkhoff fixed point theorem, between the islands in

an island-chain, there exist the hyperbolic invariant sets. And cantori are known to consist of hyperbolic invariant sets too. Therefore, when the orbits diffuse through island-chain and cantori, the corresponding hyperbolic invariant sets would slow down the speed of diffusion. So we can conclude also that the generalized stickiness effect is caused mainly by the hyperbolic invariant sets.

Acknowledgements

We are grateful to Drs. C. Efthymiopoulos, C. Froeschlé, E. Lega, R. Dvorak and H. Varvoglis for very helpful discussions and suggestions during the preparation of the manuscript. The first author thanks the IMS of CUHK in Hong Kong for the hospitality during his visit. This work is supported by the Natural Science Foundation of China (No. 10233020), the Special Funds for Major State Basic Research Project (G200077303), and a grant from the Department of Education of China for Ph.D candidate training (20020284011). The second author is also supported by the Academy of Finland (No. 44011) and NSFC (No. 10403004).

References

Chirikov B. and Shepelyansky D. L.: 1984, 'Correlation properties of dynamical chaos in Hamiltonian systems', *Physica D* **13**, 395–400.

Chirikov B. and Shepelyansky D. L.: 1999, 'Asymptotics statistics of Poincaré recurrences in Hamiltonian systems with divided phase space', *Phys. Rev. Lett.* **82**, 528–531.

Contopoulos G., Harsoula M., Voglis N. and Dvorak R.: 1999, 'Destruction of islands of stability', *J. Phys. A: Math. Gen.* **32**, 5213–5232.

Contopoulos G., Voglis N., Efthymiopoulos C., Froeschlé Cl., Gonczi R., Lega E., Dvorak R. and Lohinger E.: 1997, 'Transition spectra of dynamical systems', *Celest. Mech. Dyn. Astron.* **67**, 293–317.

Ding M., Bountis T. and Ott E.: 1990, 'Algebraic escape in higher dimensional Hamiltonian systems', *Phys. Lett. A* **151**, 395–400.

Efthymiopoulos C., Contopoulos G. and Voglis N.:, 1999, 'Cantori, islands and asympototic curves in the stickiniess region', *Celest. Mech. Dyn. Astron.* **73**, 221–230.

Efthymiopoulos C., Contopoulos G., Voglis N. and Dvorak R.: 1997, 'Stickiniess and cantori', *J. Phys. A: Math. Gen.* **30**, 8167–8186.

Froeschlé Cl. and Lega E.: 1998, 'Modelling mappings: an aim and a tool for the study of dynamical systems', In: D. Benest & Cl. Froeschlé (eds.), *Analysis and Modelling of Discrete Dynamical Systems*, pp. 3–54. The Netherlands, Gordon and Breach Science Publishers.

Karney C. F.: 1983, 'Long-time correlations in the stochastic regime', *Physica D* **8**, 360–380.

Lai Y. C., Ding M. Z., Grebogi C. and Blumel R.: 1992, 'Algebraic decay and fluctuations of the decay exponent in Hamiltonian systems', *Phys. Rev. A* **46**, 4661–4669.

Meiss J. D. and Ott E.: 1985, 'Markov-tree model of intrinsic transport in Hamiltonian systems', *Phys. Rev. Lett.* **55**, 2741–2744.

Perry A. D. and Wiggins S.: 1994, 'KAM tori are very sticky: rigorous lower bounds on the time to move away from an invariant Lagrangian torus with linear flow', *Physica D* **71**, 102–121.

Sun Y. S. and Fu Y. N.: 1999, 'Diffusion character in four-dimensional volume preserving map', *Celest. Mech. Dyn. Astron.* **73**, 249–258.

Sun Y. S., Zhou J. L., Zheng J. Q. and Valtonen M.: 2002, 'Diffusion in comet motion', *Contemporary Mathematics* **292**, 229–238.

Zhou J. L., Zhou L. Y. and Sun Y. S.: 2002, 'Hyperbolic structure and stickiness effect', *Chin. Phys. Lett.* **19**, 1254–1256.